Journal of Geography, Environment and Earth Science International
9(1): 1-8, 2017; Article no.JGEESI.27226
ISSN: 2454-7352

SCIENCEDOMAIN ***international***
www.sciencedomain.org

Investigation of Seismo-thermal Precursor of Goharan Earthquake (2013) by Thermal Data of MODIS Sensor in TERRA Satellite

Sina Saber-Mahani[1], M. Reza Sepahvand[1*] and M. Hosseinjani Zadeh[2]

[1]Department of Geophysics, Graduate University of Advanced Technology, Kerman, Iran.
[2]Department of Ecology, Institute of Science and High Technology and Environmental Science, Graduate University of Advanced Technology, Kerman, Iran.

Authors' contributions

This work was carried out in collaboration between all authors. Author SSM designed the study, wrote the protocol and wrote the first draft of the manuscript. Authors MRS and MHZ managed the literature searches and advised to author SSM. All authors read and approved the final manuscript.

Article Information

DOI: 10.9734/JGEESI/2017/27226
Editor(s):
(1) Nagendra Pratap Singh, Department of Geophysics, Banaras Hindu University, India.
(2) Ioannis K. Oikonomopoulos, Core Laboratories LP., Petroleum Services Division, Houston Texas, USA.
Reviewers:
(1) Adepelumi Adekunle Abraham, Obafemi Awolowo University, Ile-Ife, Nigeria.
(2) S. B. Ota, Institute of Physics, Sachivalaya Marg, Bhubaneswar 751005, India.
(3) Valiya M. Hamza, National Observatory, Rio de Janeiro, Brazil.
Complete Peer review History: http://www.sciencedomain.org/review-history/17633

Case Study

Received 24th May 2016
Accepted 20th July 2016
Published 27th January 2017

ABSTRACT

The main objective of this research is to study the seismo-thermal earthquake precursor of the Goharan earthquake (2013) using TERRA satellite imaging and MODIS (Moderate-resolution Imaging Spectroradiometer) sensor. In order to reach this goal, Land Surface Temperature (LST) data for seismo-thermal precursor was considered through colorization and time series analysis using wavelet transform. In addition, air effects the reduction in air temperature time series of the closest station subtracted from LST time series. Results of colorization revealed that the region with higher temperature can be used for recognition of the fault plane and the auxiliary plane. Subsequently, after plotting earthquake aftershocks, it is possible to estimate the location of the strike of the earthquake fault and the found strike location is in agreement with the higher temperature line. Also, the analysis of the time series and application of wavelet transform analysis

**Corresponding author: E-mail: mrsepahvand@yahoo.com;*
Co-author: E-mail: cna.mahani@yahoo.com;

shows that before an earthquake occurs, the soil temperature reaches the highest temperature four days prior to the event. A day before the earthquake occurs; the soil's temperature subsides to the minimum.

Keywords: MODIS; earthquake prediction; seismo-thermal precursor; LST; time-series.

1. INTRODUCTION

A significant part of Iran's territory is located in the seismic belt of the Alpine, which is an area of high seismicity. Therefore, studies should be conducted to observe the nature and characteristics of the local seismic event. The majority of strong earthquakes experience a sudden change in: the local magnetic field of the earth, animal behavior, a change in the levels of the underground water table, volcanic activity, and the appearance of earthquake clouds [1-4]. In addition, vigorous earthquakes produce mid-infrared anomaly [5-7].

Recently, new precursors have been identified, some of them based on Remote Sensing (RS) studies of the thermal infrared region. RS technology (especially space-borne sensors) is available worldwide at relatively low expenses, time, and manpower, compared to other methods. Nowadays, multiple satellites such as NOAA equipped with radiometer (AVHRR) and TERRA equipped with Spectroradiometer (MODIS) can detect mid-infrared radiation [6,8].

More acceptable answers can be provided with thermal precursors because of the thermal data that is available. Hence, this study has incorporated seismo-thermal anomaly. Thermal anomaly is commonly detected within the range of 1 to 24 days prior to the earthquake. With temperature rises to between 5 to 12°C and its effect remains after the main shock [5]. Some of the work has reported a temperature rise of 2 to 10°C [9,10]. Relations between the change in temperature and the earthquake have also been reported in investigations in Russia, China and Japan [8,11].

Also, land surface temperature (LST) depends on parameters such as: a) geographic location, b) season of year, c) radiation of sun, d) soil texture and humidity level, e) vegetation cover, and f) atmospheric condition [12]. With the exception of the last case, all of these parameters are almost constant on the same day prior to earthquake. Therefore, an abrupt change in the local air temperature is a good indicator of an upcoming earthquake. Note that other factors including volcanic activities could cause thermal anomaly. If the anomaly is caused by an earthquake then the reason for that anomaly would be a change in soil properties of further increment of stress in earth lower layers. Studies showed that several days prior to an earthquake some gas such as methane, carbon dioxide, and hydrogen are emitted from porous of soil, therefore, greenhouse gases and the magnetic field are intensified during that time [13]. Some other theories, such as piezoelectric and strain dilation, have been proposed to explain the thermal anomaly before an earthquake. However, these theories are not fully validated for seismo-thermal anomaly, thus, the precise mechanism of anomaly is questionable and poorly defined [8,14,15].

Some of remote sensing (RS) satellite (i.e. TERRA) are able to measure the land surface radiation in the thermal band. These satellites are useful for earthquake prediction due to the proper spatial and temporal resolution in the thermal band. In this paper Goharan earthquake with a Magnitude of 5.6 Mw is studied with a seismo-thermal approach by using the processing of thermal bands of MODIS sensor of TERRA satellite.

1.1 Earthquake Information

The Makran region in Iran doesn't have a good distribution of seismometer stations because of insecurity we select this earthquake because it has been efficiently documented. According to the Institute of Geophysics at the University of Tehran (IGUT), on February 2nd 2014 an earthquake with the magnitude of 5.6 in the Mw scale struck Goharan. The Epicenter's location was 26.71 N, 57.79 E and the depth of it was 5 km.

According to the Global CMT (www.globalcmt.org) solution at Harvard University, the fault type is strike slip. Also, according to National Geoscience Database of IRAN (NGDIR), the Minab fault caused this earthquake. However, through consideration of the earthquake focal mechanism, Goharan-Bashagard fault was a candidate for causative fault. Considering of foreshocks and aftershocks approves, the causative was delineated to has W-E strike.

2. DATA AND METHODOLOGY

This section is comprised of three parts. The LST and air temperature data are discussed in the first and second parts respectively. The third part reviews wavelet theory as filtering.

2.1 LST Data

In this study the LST data was obtained from two different sources, local sensing (measured at the studied location) and remote sensed data (obtained from satellite). The first set of data are local data which are obtained from thermometers that were buried in the soil at varying depths (5, 10, 20, 30, 50 and 100 cm). The temperature data of those sensors are recorded at 3:00, 9:00 and 15:00 (Local Time). The location of each sensor along with the time and depth of the sensors are logged in the data. The most favorable depth for placing the sensor for seismo-thermal precursor detection purpose is 100 cm, because it receives the lowest impact from surface parameters. The second set of LST data belongs to data that was obtained from meteorology satellites. It is possible to extract temperatures from the satellites data, which record Land Surface Radiation (LSR) in thermal infrared region. In addition, geostationary stations record LST every 30 minutes. Also, the three satellites NOAA, TERRA and AQUA record LST twice a day.

The Moderate Resolution Imaging Spectroradiometer (MODIS) onboard the Terra satellite, was launched on December 18, 1999 for global monitoring of the atmosphere, terrestrial ecosystems, and oceans. MODIS with its 2330 km swath width provides almost complete dual global daily coverage in 36 spectral bands between 0.415 and 14.235 µm with spatial resolutions of 250 m (bands 1 and 2), 500 m (bands 3, 4, 5, 6 and 7) and 1000 m (bands 8–36) [16]. In this study, LST variations near the epicenter of the studied earthquake have been analyzed using the daytime LST images provided by NASA (http://modis.gsfc.nasa.gov/data). These data were generated on a daily basis at a temperature resolution of 0.02 K. Each pixel of a LST image covers an area of 1×1 km^2 on the ground. For each image, the average of LST values of a 3×3 pixel area centered on the earthquake epicenter was used.

2.1.1 Air temperature data

Air Temperature (AT) data was obtained from Wunderground web site (http://www.wunderground.com/) from January 16 to February 12 in 4 years 2011-14. The data was recorded by the meteorological stations close to the studied earthquake's epicenter. Fig. 1 shows the average of 3 years AT time series subtracted from 2014's AT time series of Darshahr station. It has been argued that LST nighttime of MODIS sensor is proportional to the minimum temperature of the day [11].

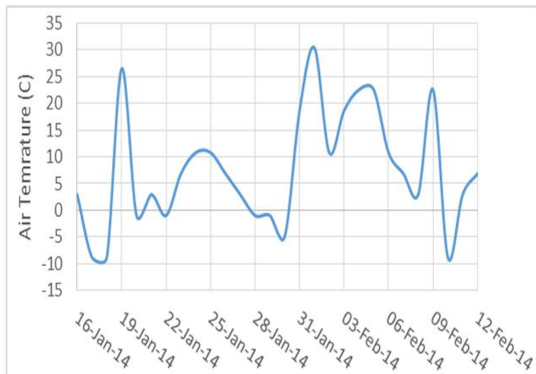

Fig. 1. Average of 3 years AT subtracted from 2014's AT time series at closest station to epicenter

2.2 Anomaly Detection by Wavelet Transform

The wavelet transformation technique (Equation 1) has been applied on the LST time series of earthquakes to obtain the time variability of the main periodicities. Similarity to Short Time Fourier Transform (STFT) for performing wavelet transform on data, signal (in this article, LST time series) product to wavelet function that in reality it has the same role of window function.

$$\psi(a,b)=\frac{1}{\sqrt{|a|}}\int_{-\infty}^{+\infty}x(t)\,\psi^{*}\left(\frac{t-b}{a}\right)dt \quad (1)$$

Where, 'a' is the scaling factor, 'b' is the location parameter, ψ^{*} is the complex conjugate of continuous wavelet functions and f(x) is the time series under analysis [17].

Here, Haar wavelet or daubechies-1 wavelet is used. Significant correspondence between signal (time series) and daubechies family wavelets is the main reason for selecting this method. According to what is stated in preceding studies, thermal anomaly has a peak and then a valley; daubechies wavelets have also the same shape. More correlations between signal and wavelet results a higher signal to noise ratio (SNR) [18].

3. PROCESSING AND INTERPRETATION

A visual analysis of thermal images followed by a detailed analysis was carried out to determine the approximate location of appearance of a thermal anomaly, intensity of thermal rise, and its spatial extent. Since MODIS cannot penetrate through clouds, cloudy areas will give the temperature of the cloud top and not the actual LST of the area. Therefore pixels with cloudy cover were excluded from the image. For preparation of time series LST maps the datasets were treated identically and a user-specified temperature range consistent for all scenes of a particular earthquake was defined to distinctly delineate the thermal anomalous area. By applying the above mentioned modifications and making LST time series map with these maps, the effect of seismo-thermal precursor are emerged as shown in Fig. 2.

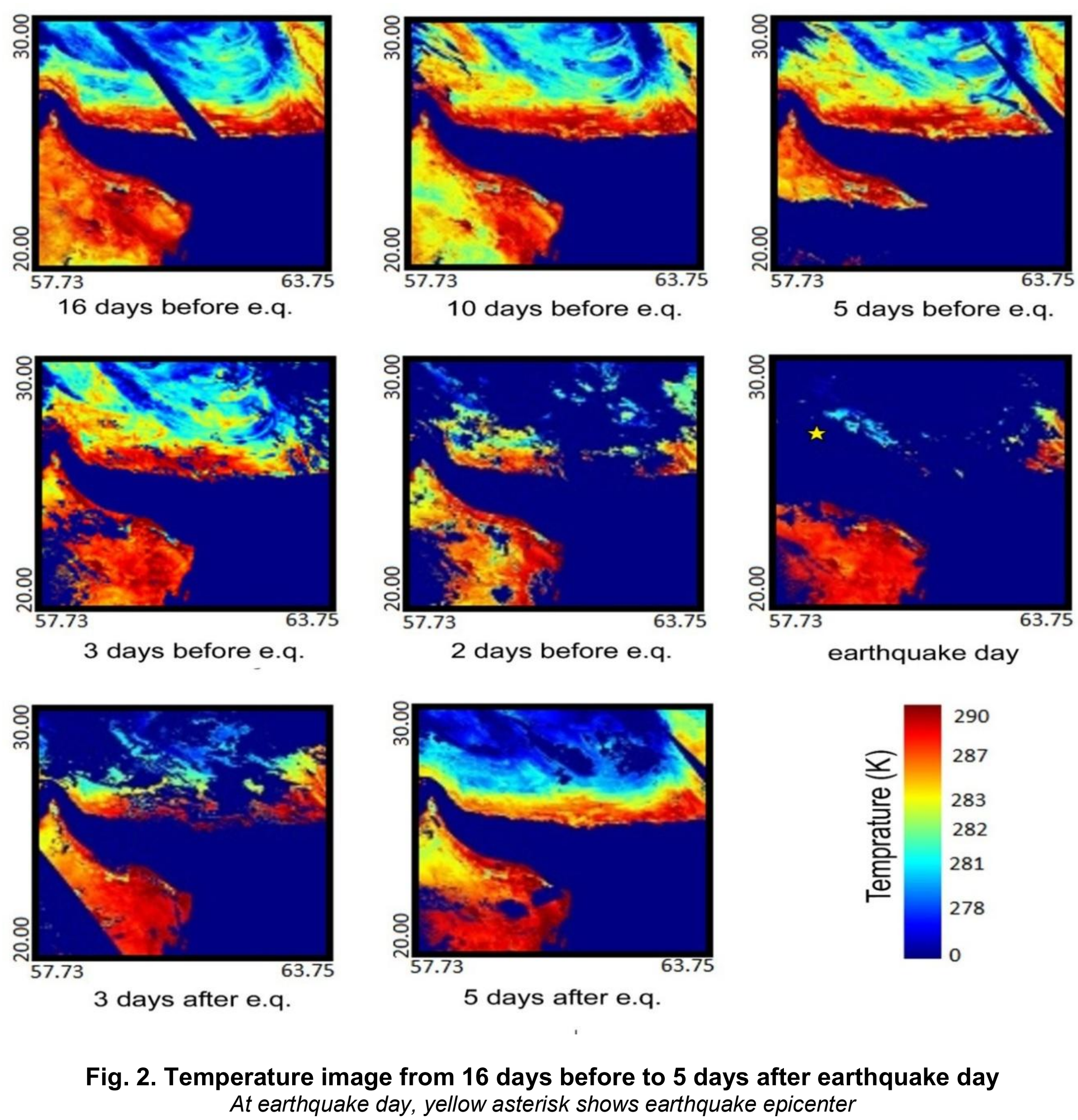

Fig. 2. Temperature image from 16 days before to 5 days after earthquake day
At earthquake day, yellow asterisk shows earthquake epicenter

Investigation of a series of satellite images of Goharan earthquake through color mapping reveals a distinct increase in temperature around the epicenter (Fig. 2). Fig. 2 clearly shows high temperature above the epicenter, several days before earthquake. However, there is no information a day prior the earthquake due to the cloud coverage at the study area. Obviously chaotic LST before main shock returned to normal condition 5 days after earthquake and temperature decreased from coast to land gradually.

Active faults, foreshocks and aftershocks were overlaid on the temperature image on Fig. 3. According to this figure, a correlation between faults and region of high temperature and quakes can be inferred. High temperature lines which were placed above of the Strike of caused fault conforms that. Also, the high temperature line is inside of the effective region that was introduced by Dobrovolsky [19]. The effective radius of Goharan earthquake was calculated by equation 2. According to the result, Goharan's effective radius is 255.85 km – it covered high temperature line. (< not sure on this part. Depends on what you want to imply.)

$$R = 10^{0.43M} \tag{2}$$

At the second part, the data was investigated by time series analysis. In order to reduce the effect of the noise and inaccuracy caused by the presence of clouds, the LST data of the epicenter pixel and 8 closest pixels was used (Fig. 4). Therefore, an average of 9 pixels was considered as the temperature of the day for each location. Previous studies show that the temperature around a rupture zone decreases logarithmically with distance [20], so iregards to pixels close to each other, this approach subsides error more sufficiently than considering only the/an epicenter pixel.

Goharan temperature time series is extracted from 16 days prior to earthquake to 10 days after it (Fig. 5). Earthquake day is considered as indicating zero in the time axis.

From the time series curve, it is obvious that a sudden (word missing.) in temperature was noted 3 days prior to the earthquake an occurrence and then decreases 1 day after earthquake. After this decline, the temperature was observed to return to a normal condition that was previously maintained.

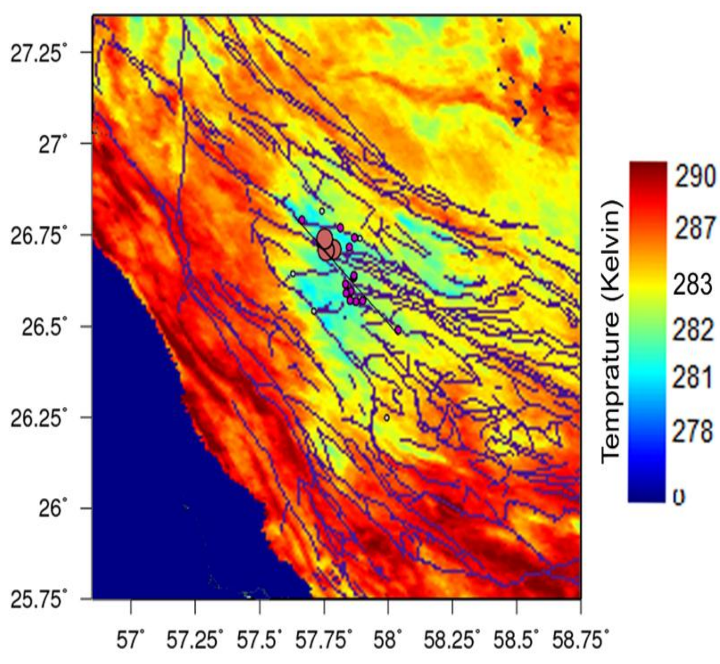

Fig. 3. Temperature image with active faults (Blue solid lines). Foreshocks, aftershock and main shock (purple circles) are illustrated in this figure
Black lines indicates an inferred fault

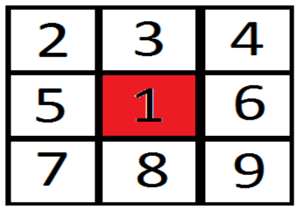

Fig. 4. Square array for extracting LST data.
Pixel number 1 matches to epicenter

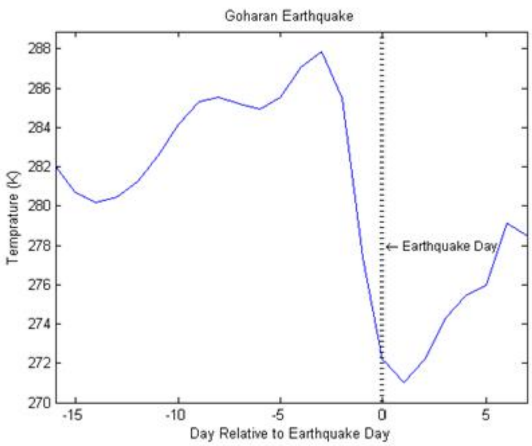

Fig. 5. LST time series of Goharan earthquake

By subtracting the AT time series from the LST, the effects of air conditioning are reduced dramatically. Since other effective parameters of LST for the same earthquake are constant, their effects are negligible.

Because of keeping a real range of LST time series, an average value of AT time series was observed to be reduced from AT time series and the residual of this process reduced from LST time series (Fig. 6).

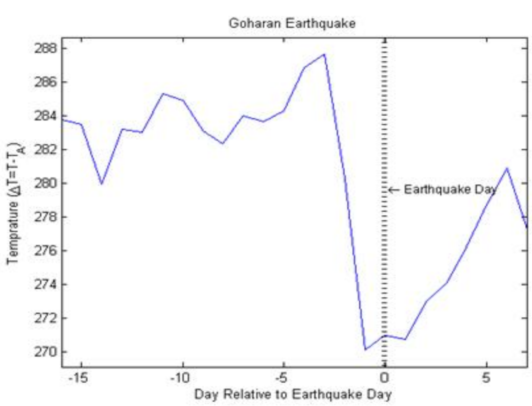

Fig. 6. Pure LST time series. In this curve, AT time series subtracted from LST time series

During the process of filtering the time series, a stationary wavelet transformation was used to keep the length of the signal. Here Haar function was selected as the most applicable wavelet to be employed. Wavelet at 3 levels was performed on time series, then the thresholding process was applied on the filtered time series. After performing wavelet transform original and the filtered signals were plotted in Fig. 7.

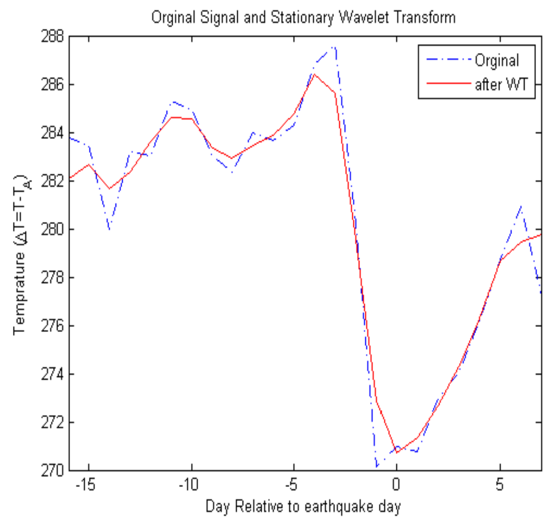

Fig. 7. Performing wavelet transform on time series
The curve in red is filtered curve and the dotted curve in blue is the original curve before performing filtration

According to LST time series, the temperature is at normal 8 days prior to earthquake and it reaches a maximum of 4 days before the occurrence of the earthquake. Thereupon, it sharply decreases to the/a minimum on the earthquake day. After this drop in temperature, the time series curve returns to background level. Wavelet filtering removes the effect of noise from the modified time series curve and produces a smooth curve for better interpretation.

4. DISCUSSION AND CONCLUSION

Detail location prediction, seismo-thermal prediction and time prediction was carried for the earthquake prediction using colorization images (Fig. 2), high temperature and time-series analysis. The results obtained confirm the efficacy of this method for earthquake predictions and monitoring.

Fig. 2 shows the existence of a high temperature region in the west of Makran seismotectonic zone. This zone increased in temperature in days prior to the main quake and decreased several days after that.

In Fig. 3, an admirable correlation is present between the seismo-precursor, thermal properties (high temperature) and the fault zone investigated. It was observed that the high temperature zone disappears days after the occurrence of the earthquake. In result, we can infer that the sudden rise and fall of the temperature is possibly related to the earthquake. Through the methodology adopted for this study, we have been able to establish the relationship between the occurrence of the earthquake, the temperature and the fault zone. In other zones of the map, faults have a vast correspondence with high temperature lines. Moreover, for the considered earthquake, aftershocks conform strike of caused faults.

In other parts of article, the LST time series of the Goharan earthquake survived by the usage of a wavelet filter. Furthermore, air temperature circulation is applied on the LST time series. This application is done because we want to remove the air effect; by doing so, we somewhat ensure that the anomaly behavior in the investigation is NOT due to change in the climate condition.

The wavelet used was able to eliminate the high frequency of noise existing in the area. The high surface temperature is directly related to the period when the Goharan earthquake occurred. Nevertheless, the minimum temperature entity was observed a few days after the occurrence of the earthquake. However, we believe that the reason could be independent of the earthquake.

COMPETING INTERESTS

Authors have declared that no competing interests exist.

REFERENCES

1. Habarulema JB, Mckinnell LA, Opperman BDL. TEC measurements and modelling over Southern Africa during magnetic storms; a comparative analysis. Journal of Atmospheric and Solar Terrestrial Physics. 2010;72(5-6):509-520.
2. Meloni A. Tectonomagnetics and VLF electromagnetics signal in central Italy. Annals of Geophysics. 2009;47.
3. Yamaguchi R, Otaka S. Precursory changes in water level at Funabara and Kakigi before the Izu-Oshima-Kikai earthquake of 1978. Bull. Earthquake Res. Inst. Univ. Tokyo. 1978;53:841–854.
4. Shuguang Q, Guangmeng G. Clouds anomaly before Italy 6.0 earthquake. EMSEV 2012. Gotemba Kogen Resot, JAPAN. 2012;1-11.
5. Saraf AK, Rawat V, Choudhury S, Dasgupta S, Das J. Advances in understanding of the mechanism for generation of earthquake thermal precursors detected by satellites. International Journal of Applied Earth Observation and Geoinformation. 2009;9: 373–379.
6. Saraf AK, Rawat V, Banerjee P, Choudhury S, Panda SK, Dasgupta S. Satellite detection of earthquake thermal infrared precursors in Iran. Natural Hazard. 2008;47:119-135.
7. Mahani SS. Applying LDF such an Innovative method on time series of soil temperature in earthquake prediction. Journal of Tethys. 2016;4:12-17.
8. Ouzounov D, Freund F. Mid-infrared emission prior to strong earthquakes analyzed by remote sensing data. Elsevier; 2004.
9. Saraf AK, Choudhury S. Thermal remote sensing technique in the study of pre-earthquake thermal anomalies. J. Ind. Geophys. Union. 2005;9:197-207.
10. Saradjian MR, Akhoondzadeh M. Prediction of the date, magnitude and affected area of impending strong earthquakes using integration of multi precursors earthquake parameters. Natural Hazards and Earth System Science; 2011.
11. Leptoukh G, Shen S. Estimation of surface air temperature over central and eastern Eurasia from MODIS land surface temperature. Environmental Research Letters. 2011;6:8-10.
12. Arya SP. Introduction to micrometeorology. Second ed.: Academic Press; 1998.
13. Zuji Q, Xiudeng X, Changgong D. Thermal anomaly-precursor of impending earthquake. Chinese Science Bulletin. 1990;35(17):1324-1327.
14. Ouzounov D, Freund F. Ground atmosphere-ionosphere interaction related to earthquake: How can Earthquake help?. SCEC Publication; 2001.
15. Eleftheriou A, Filizzola C, Genzano N, Lacava T, Pergola N, Tramutoli V. Long-term RST analysis of anomalous TIR sequences in relation with earthquakes

occurred in greece in the period 2004-2013. Pure and Applied Geophysics. 2016; 173:285-303.
16. Wan Z. MODIS land surface temperature products users' guide. ICESS, University of California, Santa Barbara (Users' Guide); 2006.
17. Fugal DL. Conceptual wavelet in digital signal processing. Space & Signal Technical Publishing; 1994.
18. Baili J, Samer Lahouar, Hergli M, Al-Qadi I, Kamel Besbes. GPR signal de-noising by discrete wavelet transform. NDT & E International. 2009;42:696–703.
19. Dobrovolsky IR, Zubkov SI, Myachkin VI. Estimation of the size of earthquake preparation zones. Pure Appl. Geophys. 1979;77:1025-1044,.
20. Askari G, Hafezi-Moghaddas N, Rahimi-tabar MR, Ansari A. Detection of thermal infrared (TIR) anomalies related to the Ms=5.1 earthquake on Oct.14, 2004 near Ravar (SE Iran). Journal of the Earth and Space Physics. 2010;35:1-16.

Peer-review history:
The peer review history for this paper can be accessed here:
http://sciencedomain.org/review-history/17633